L ETTER TO THE E DITOR

H I Observations of two New Dwarf Galaxies: Pisces A & B with the SKA Pathfinder KAT-7

C. Carignan[1,2] ⋆, Y. Libert[1], D. M. Lucero[1,3], T. H. Randriamampandry[1], T. H. Jarrett[1],
T. A. Oosterloo[3,4], and E. J. Tollerud[5]

[1] Department of Astronomy, University of Cape Town, Private Bag X3, Rondebosch 7701, South Africa
[2] Observatoire d'Astrophysique de l'Université de Ouagadougou, BP 7021, Ouagadougou 03, Burkina Faso
[3] Netherlands Institute for Radio Astronomy (ASTRON), Postbus 2, 7990 AA Dwingeloo, The Netherlands
[4] Kapteyn Astronomical Institute, University of Groningen, PO Box 800, 9700 AV Groningen, The Netherlands
[5] Space Telescope Science Institute, 3700 San Martin Dr, Baltimore, MD 21218, USA

January 5, 2016

ABSTRACT

Context. Pisces A & Pisces B are the only two galaxies found via optical imaging and spectroscopy out of 22 H I clouds identified in the GALFAHI survey as dwarf galaxy candidates.
Aims. Derive the H I content and kinematics of Pisces A & B.
Methods. Aperture synthesis H I observations using the seven dish Karoo Array Telescope (KAT-7), which is a pathfinder instrument for MeerKAT, the South African precursor to the mid-frequency Square Kilometre Array (SKA-MID).
Results. The small rotation velocities detected of ~5 km s^{-1} and ~10 km s^{-1} in Pisces A & B respectively, and their H I content show that they are really dwarf irregular galaxies (dIrr). Despite that small rotation component, it is more the random motions ~ 9-11 km s^{-1} that provide most of the gravitational support, especially in the outer parts. The study of their kinematics, especially the strong gradients of random motions, suggest that those two dwarf galaxies are not yet in equilibrium.
Conclusions. These H I rich galaxies may be indicative of a large population of dwarfs at the limit of detectability. However, such gas-rich dwarf galaxies will most likely never be within the virial radius of MW-type galaxies and become sub-halo candidates. Systems such as Pisces A & B are more likely to be found at a few Mpc.s from MW-type galaxies.

Key words. techniques: interferometric – galaxies: dwarf – galaxies: ISM – galaxies: Local Group

1. Introduction

Optical searches for faint dwarf galaxies and satellites (dSph or dIrr) are generally surface brightness limited. While having some success recently for very nearby dwarfs in deep optical surveys, such as the Dark Energy Survey (Koposov et al. 2015) and the PAN-STARRS 1 3π Survey (Laevens et al. 2015), the task becomes very difficult as soon as one gets further out in the Local Volume (5-10 Mpc). This was shown clearly with the discovery of seven dwarf galaxies close to M101, which have central surface brightnesses of $\mu_g \sim 25.5 - 27.5$ mag arcsec^{-2}, well below the sky brightness, and was only possible through the development of a new instrument, the Dragonfly Telephoto Array (Merritt, van Dokkum & Abraham 2014).

This motivates searches for dwarf galaxies using the 21cm emission line of neutral hydrogen (H I). While such searches cannot identify passive dwarf galaxies (dSph) like most Local Group satellites, which lack H I (M$_{HI}$/L$_V \leq 10^{-3}$ M$_\odot$/L$_\odot$: Spekkens et al. 2014), they have the potential to find gas-rich, potentially star-forming dwarf (dIrr) galaxies (see e.g. Adams, Giovanelli & Haynes 2013; Adams et al. 2015; Cannon et al. 2015; Janowiecki et al. 2015).

Good examples are the dwarf galaxies Leo P, found first in H I (Giovanelli et al. 2013) and later confirmed by optical imaging (Rhode et al. 2013) and Leo T, first detected in H I by HIPASS

(Wong et al. 2006) but discovered independently in the optical a year later by Irwin et al. (2007). However, those galaxies detected in H I cannot aleviate the Missing Satellite Problem and be sub-halos candidates, since, for example, Leo T at ~400 kpc (McConnachie 2012) is outside the virial radius of the Milky Way (MW) and Leo P at ~ 1.5-2.0 Mpc (McQuinn et al. 2013) is well outside the Local Group. Possible sub-halos, that could be associated to the MW or M31, are more likely dSphs stripped of their gas (Grcevich & Putman 2003) or completely "dark" systems (Brooks et al. 2013).

Tollerud et al. (2015), hereafter TOL15, report the discovery of two dwarf galaxies, Pisces A and B, from a blind 21cm H I search. These were the only two galaxies found via optical imaging and spectroscopy (WIYN) out of 22 H I clouds identified in the GALFAHI survey (Peek et al. 2011) as dwarf galaxy candidates. While the distance uncertainty made any interpretation ambiguous at the time, TOL15 propose that they are likely winthin the Local Volume (< 10 Mpc) but outside of the Local Group (> 1 Mpc). They also suggest that they may be among the faintest star-forming dwarf galaxies known.
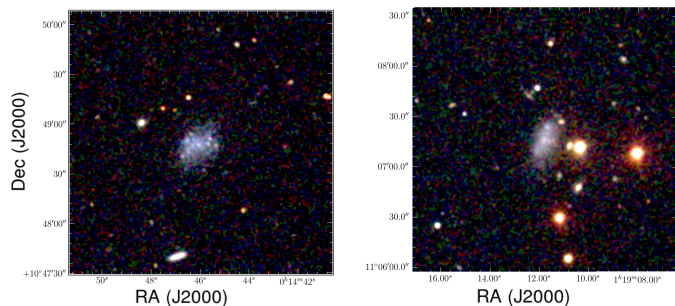
Fig. 1 shows SDSS (gri) images of Pisces A and B. The fact that the brightest stars are being resolved in Pisces A already suggests that it is most likely closer than Pisces B. Table 1 summarizes the parameters of the two new dwarf galaxies, using the new determined distances of Tollerud et al. (2016). The remainder of this letter is as follows. Sect. 2 gives a description of the

⋆ ccarignan@ast.uct.ac.za

Table 1. Parameters of Pisces A and B.

Parameter	Pisces A	Pisces B
R. A. (J2000)	00^h 14^m 46.0^s	01^h 19^m 11.7^s
Dec. (J2000)	$+10^o$ $48'$ $47''$	$+11^o$ $07'$ $18''$
l (^{o})	108.52	133.83
b (^{o})	-51.03	-51.16
Axis ratio (q=b/a)	0.60	0.45
Inclination (^{o})	53±5	63±5
P. A. (^{o})	111±3	156±1
NUV (mag)	19.18±0.13	18.80±0.06
m_r (mag)	17.37±0.19	17.19±0.16
$(g - r)$ (mag)	0.24	0.31
Distance (Mpc)[a]	5.6±0.2	8.9±0.8
Scale (kpc/arcmin)	1.6	2.6
$r_{\rm eff,major}$ (pc)[a]	145^{+5}_{-6}	323^{+27}_{-30}
M_V (abs. mag)[a]	$-11.57^{+0.06}_{-0.05}$	$-12.90^{+0.2}_{-0.2}$
log $(M_{*,\,SFH} / M_\odot)$[a]	$7.0^{+0.4}_{-1.7}$	$7.5^{+0.3}_{-1.8}$

(a) Tollerud et al. (2016)

Fig. 1. SDSS combined gri images of Pisces A (left) & B (right).

Table 2. Parameters of the KAT–7 observations.

Parameter	Pisces A & B
Start of observations	27 November 2014
End of observations	16 December 2014
Total integration	26.5 & 24.0 hours
FWHM of primary beam	1.27°
Total Bandwidth	12.5 MHz
Central frequency	1419.3 & 1417.5 MHz
Channel Bandwidth	15.0 kHz
Channel width	3.2 km s^{-1}
Maps gridding	15″ x 15″
Maps size	512 x 512
Flux calibrator	1934-638
Phase/bandpass calibrator	0022+002
Robust = 0 weighting function	
FWHM of synthesized beam	283″x 184″& 284″x 181″
RMS noise (mJy/beam)	4.5 & 4.2
Column density limit	
(3σ over 16 km s^{-1})	$\sim 5 \times 10^{18}$ cm^{-2}
Natural weighting function	
FWHM of synthesized beam	320″x 203″& 316″x 200″
RMS noise (mJy/beam)	3.4 & 3.2
Column density limit	
(3σ over 16 km s^{-1})	$\sim 2.5 \times 10^{18}$ cm^{-2}

on the observed calibrators suggest that the absolute flux uncertainties are on the order of 5%. Variations in the bandpass are on the order of 1%.

Continuum emission was subtracted from the raw UV data by making first order fits to the line free channels using the CASA task uvcontsub. The calibration was then applied and Pisces A and B were split from the calibration sources. KAT-7 does not use doppler tracking and CASA does not fully recognize frequency keywords, so special care was taken to produce uv data sets and test cubes with the proper velocity coordinates (see Carignan et al. 2013). The individual calibrated continuum subtracted UV data sets were then combined together using the CASA task concat.

Preliminary imaging of the combined data in CASA revealed the presence of artifacts in the form of horizontal lines, caused by some unidentified internal instrumental feature. At the suggestion of T. A. Oosterloo, these were removed by flagging all visibilities near u = 0 (see also Hess et al. 2015), clearly seen to be out of range after performing an FFT on the images. Careful data analysis also allowed us to discover and correct for an artifact caused by *crosstalk* between two antennas. This occurs when one antenna is pointing towards the back of another at an elevation high enough to prevent the shadowing flag to be triggered by the system, but low enough to produce strong variations in the bandpass.

Karoo Array Telescope (KAT-7) observations and data reduction, Sect. 3 describes the Hi content and kinematics of Pisces A and B, the main results are discussed in Sect. 4 and Sect. 5 presents the final conclusion.

2. KAT-7 Observations and Data Reduction

The observations were obtained with the seven-dish KAT-7 array (Carignan et al. 2013; Lucero et al. 2015), located close to the South African SKA core site in the Northern Cape's Karoo desert region. The array is extremely compact, with baselines ranging from 26 m to 185 m and receivers having a very low $T_{sys} \sim 26$ K, which makes it very sensitive to large scale, low surface brightness emission. The parameters of the KAT-7 observations are given in Table 2. The data were collected between 2014 November 27 and 2014 December 16 in the c16n13M4K spectral line mode. This correlator mode gives velocity channels of 0.64 km s^{-1} over a flat bandpass of $\sim$2000 km s^{-1}. When producing the final cubes, we averaged 5 channels for a final channel width of 3.2 km s^{-1}.

Each of the observing sessions, of typically 6 hours, were reduced separately. All data calibration was done using standard calibration tasks in the Common Astronomy Software Applications (CASA 4.2.0) package (McMullin et al. 2007). Phase drifts as a function of time were corrected by means of a nearby point source (0022+002) observed every 30 minutes. This source was also used to correct for variations in the gain as a function of frequency (bandpass calibration). The absolute flux scale was set by observing 1934-638. Comparisons of the flux measurements

3. Hi Content and Kinematics

The total Hi distribution maps of Pisces A & B, shown in Figure 2, were derived using the task sqash in AIPS (Greisen 2003). They are superposed on the WISE (w1+w2+w3) and Galex (NUV) images. As expected, not much IR flux is seen in the WISE images due to the absence of an appreciable old stellar population (Pisces A is not detected in WISE, but Pisces B is, which suggests it has a larger stellar mass) but the two star-forming dwarfs are clearly seen in the UV. The faintest level goes down to $\sim$3 $\times 10^{18}$ cm^{-2}. At that level, the galaxies have
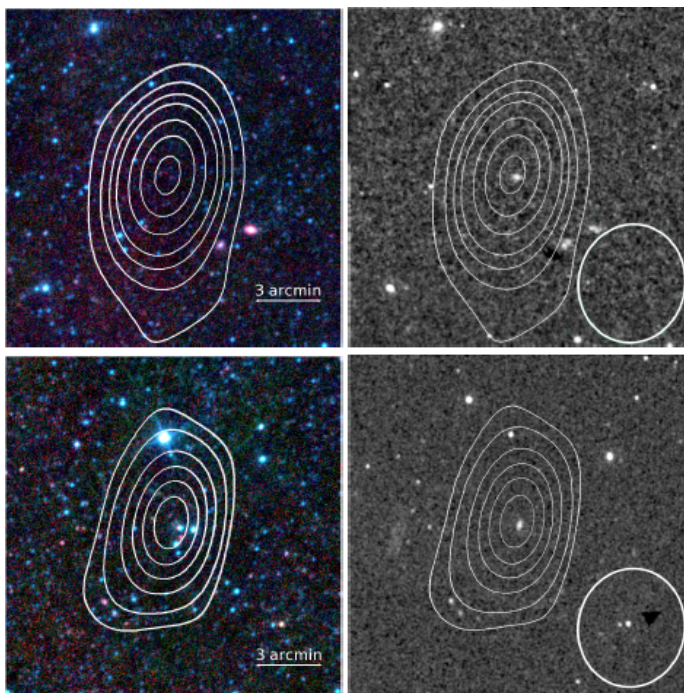
Fig. 2. H<small>I</small> distributions in Pisces A (top) and Pisces B (bottom), superposed on the 3-color WISE w1+w2+w3 composite (left) and Galex NUV (right) images, from the natural weighted cubes. Contours are at 0.3 (3 σ), 0.6, 1.2, 1.8, 2.4 and 3.0 $\times10^{19}$ cm^{-2}.

diameters of ~9.6′ and ~8.5′, respectively. Despite the large synthesized beam (see Table 2), due to the northern declinations of the sources, there are still ~2-3 beams across the objects, which is sufficient to detect any significant velocity gradient.

The global H<small>I</small> profiles are given in Figure 3. They were obtained using the task BLSUM in AIPS. Mid-point velocities (50% level) of 233±3 km s^{-1} and 617±3 km s^{-1} are found for Pisces A and Pisces B, respectively. These can be compared to 236±0.5 km s^{-1} and 615±1 km s^{-1} found by TOL15. The profile widths at the 50% levels are $\Delta V_A = 28 \pm 3$ km s^{-1} and $\Delta V_B = 41 \pm 3$ km s^{-1}, compared to $\Delta V_A = 22.5 \pm 1.3$ km s^{-1} and $\Delta V_B = 43 \pm 3$ km s^{-1} for TOL15. Total H<small>I</small> fluxes of 1.68 ± 0.20 and 1.76 ± 0.05 Jy km s^{-1} are found, which correspond to H<small>I</small> masses of 4.0 ± 0.5 $\times10^5$ M$_\odot$ and $4.2 \pm 0.2 \times10^5$ M$_\odot$ at a fiducial distance of 1.0 Mpc. This is slightly larger than the values of $2.8 \pm 0.2 \times10^5$ M$_\odot$ and $3.8 \pm 0.4 \times10^5$ M$_\odot$ found by TOL15. At the adopted distance, this corresponds to total H<small>I</small> masses of $1.3 \pm 0.4 \times 10^7$ & $3.3 \pm 1.0 \times 10^7$ M$_\odot$ for Pisces A & B.

It is difficult to understand the difference for Pisces A (~30% in flux and ~20% in width), while both data sets agree perfectly in the case of Pisces B, since the same calibrators and techniques were used for both objects. Comparing the global profiles, the difference is clearly on the approaching side. However, we are quite confident in the width derived for Pisces A since the value obtained by TOL15 would imply that no rotation is present, while rotation is clearly seen in the velocity field of Pisces A (Fig. 4).

From the moment analysis, derived with the task MOMNT in AIPS, the mean σ (random motion) of the H<small>I</small> is 9.4 ± 2.0 km s^{-1} for Pisces A and 11.0 ± 3.7 km s^{-1} for Pisces B. For Pisces A, there is a gradient from ~6 km s^{-1} in the North to ~12 km s^{-1} in the South and for Pisces B from ~15 km s^{-1} in the center down to ~7 km s^{-1} at the edge of the disk. The global profiles show that some rotation is clearly present of the order of $(7 \pm 3)/2(\sin i)\sim$
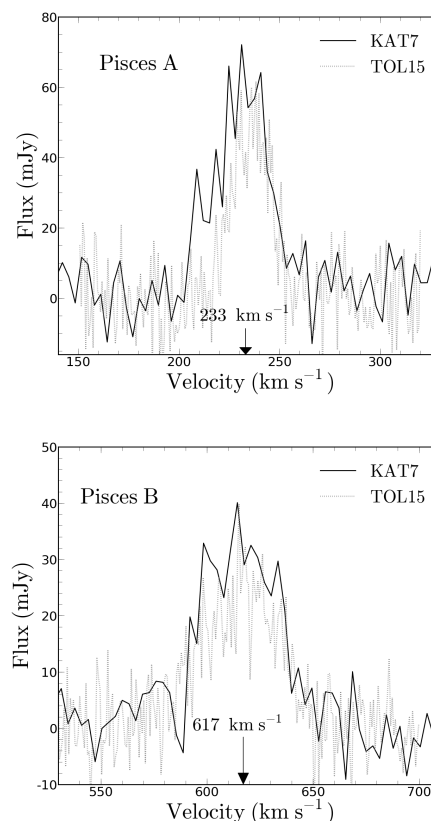

Fig. 3. Global H<small>I</small> profiles of Pisces A (top) and Pisces B (bottom), using the natural weighted cubes. Velocities are heliocentric. The grey profiles are those from TOL15.

Table 3. H<small>I</small> parameters of Pisces A and B.

Parameter	Pisces A	Pisces B
F_{HI} (Jy km s^{-1})	1.7 ± 0.2	1.8 ± 0.1
M_{HI} (M$_\odot$)	$4.0 \times 10^5 D^2_{Mpc}$	$4.2 \times 10^5 D^2_{Mpc}$
M_{HI} (M$_\odot$)	$1.3 \pm 0.4 \times 10^7$	$3.3 \pm 1.0 \times 10^7$
M_{HI}/L_V (M$_\odot$/L$_\odot$)	4.6	3.8
D_{HI} (10^{19} cm^{-2})	11.7 kpc (7.2′)	17.4 kpc (6.7′)
D_{HI} (3×10^{18} cm^{-2})	15.6 kpc (9.6′)	22.1 kpc (8.5′)
V_{sys} (km s^{-1})	233 ± 3	617 ± 3
ΔV_{50} (km s^{-1})	28 ± 3	41 ± 3
V_{max} (km s^{-1})	4.6 ± 2.0	9.4 ± 2.1
σ (km s^{-1})	9.4 ± 2.0	11.0 ± 3.7

4.6 ± 2.0 km s^{-1} and $(17 \pm 3)/2(\sin i) \sim 9.4 \pm 2.1$ km s^{-1} for Pisces A & B. This is exactly what is seen in the velocity fields of Fig. 4, obtained by Gaussian profile fitting using the task XGAUS in AIPS. The derived H<small>I</small> parameters are given in Table 3.

4. Discussion

What we can see from the derived velocity fields is that, while the disks are fairly regular on the approaching (blue) sides, they are strongly warped on the receding (red) sides. This asymmetry, combined with the strong gradient of velocity dispersion, shows clearly that those disks are not yet in equilibrium. An alternative scenario could be that some minor amount of accretion is happening in the outer regions, while the inner disks are fairly well in equilibrium. Pisces A & B are among the few non-elliptical (non-dSph) systems known at $M_B \sim -11$, such as GR8
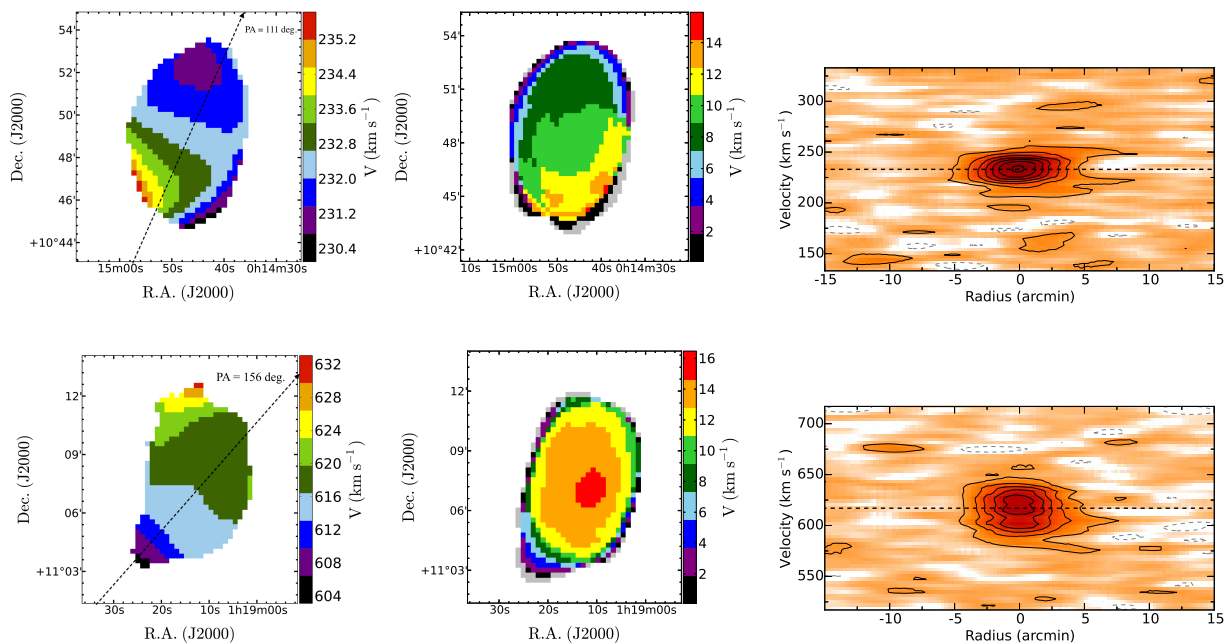
Fig. 4. Velocity fields (the dashed line shows the optical PA) from Gaussian profiles fitting (left), velocity dispersion from moment analysis (center) and PV diagrams of the hanning smoothed data for Pisces A (top) and Pisces B (bottom), where the dashed lines show the systemic velocities.

(Carignan, Beaulieu & Freeman 1990) in the Local Group and M81dwA (Sargent, Sancisi & Lo 1983) where, while rotation is providing some gravitational support in the inner parts, random motions provide essentially all the support in the outer parts. M81dwA has a rotation ~3 km s^{-1} similar to Pisces A and GR8 has a rotation of ~8 km s^{-1} of the same order as Pisces B.

When the KAT-7 H I observations started, the distances to Pisces A & B were unknown. Now that the distances are known, it is clear that those galaxies are not candidates for sub-halos of more massive MW-type galaxies. In the case of more likely sub-halo candidates, such as the 9 ultra faint dwarfs (UFD) uncovered by the Dark Energy Survey (Koposov et al. 2015), none of them were detected in H I (Westmeier et al. 2015).

Knowing the distances also revealed that Pisces A & B are quite different from Leo T & P, despite very similar HI fluxes. In fact, they are both much brighter with absolute V magnitude of −11.57 and −12.90, compared to −7.1 (Irwin et al. 2007) and −9.3 (Rhode et al. 2013) and have a much larger H I content of a few ×10^7 M$_\odot$, compared to a few ×10^5 M$_\odot$ for the less distant Leo T and Leo P.

5. Conclusion

All isolated dwarfs (i.e. those that are not satellite of a larger galaxy such as the Milky Way or M31) are actually richer in cold gas than larger galaxies (Geha et al. 2012) and, in fact, the smaller such isolated dwarfs are, the richer in cold gas they become (Huang et al. 2012). Some recent theoretical work (see e.g.: Bovill & Ricotti 2011a,b) does indeed suggest that an extensive population of yet undiscovered gas-dominated, or even dark, dwarfs may exist in the outer fringes of the Local Group or just beyond.

An examination of the dwarf galaxies within the full AL-FALFA population in the context of global star formation (SF) laws (Huang et al. 2012) is consistent with the general assumptions that gas-rich galaxies have lower SF efficiencies than do optically selected populations and that H I disks are more extended than stellar ones. Pisces A & B are good examples of this.

References

Adams. E. A. K., Giovanelli, R. & Haynes, M.P. 2013, ApJ, 768, 77
Adams. E. A. K. et al 2015, A&A, 573, L3
Bovill, M. S.& Ricotti, M. 2011a, ApJ, 741, 17
Bovill, M. S.& Ricotti, M. 2011b, ApJ, 741, 18
Brooks, A. M., Kuhlen, M., Molotov, A. & Hooper, D. 2013, ApJ, 765, 22
Cannon, J. M. et al. 2015,AJ, 149, 72
Carignan, C., Frank, B. S., Hess, K. M., Lucero, D. M., Randriamampandry, T. H., Goedhart, S. & Passmoor, S. S. 2013, AJ, 146, 48
Carignan, C., Beaulieu, S. & Freeman, K. C. 1990, AJ, 99, 1
Geha, M., Blanton, M. R., Yan, R. & Tinker, J. L. 2012, ApJ, 757, 85
Giovanelli et al. 2013, AJ, 146, 15
Grcevich, J. & Putman, M. E. 2009, ApJ, 696, 385
Greisen, E. W., 2003, Astrophysics and Space Science Library, 285, 109
Hess, K. M., Jarrett, T., Carignan, C., Passmoor, S. S., Goedhart, S. 2015, MNRAS, 452, 1617
Huang, S., Haynes, M. P., Giovanelli, R., Brinchmann, J., Stierwalt, S. & Neff, S. G. 2012, AJ, 143, 133
Irwin, M. J. et al. 2007, ApJ, 656, L13
Janowiecki, S. et al. 2015, ApJ, 801, 96
Koposov, S. E., Belokurov, V., Torrealba, G. & Evans, N. W. 2015, ApJ, 805, 130
Laevens, B. P. M. et al. 2015, arXiv:1507.07564
Lucero, D. M., Carignan, C., Elson, E. C., Randriamampandry, T. H., Jarrett, T. H., Oosterloo, T. A. & Heald, G. H. 2015, MNRAS, 450, 3935
McConnachie, A. W. 2012, AJ, 144, 4
McMullin, J. P., Waters, B., Schiebel, D., Young, W. & Golap, K. 2007, ASP Conference Series, 376, 127
McQuinn, K. B. W. et al 2013, AJ, 146, 145
Merritt, A., van Dokkum, P. & Abraham, R. 2014, ApJ, 787, L37
Peek, J. E. G. et al. 2011, ApJS, 194, 20
Rhode, K. L. et al. 2013, AJ, 145, 149
Sargent, W. L. W., Sancisi, R. & Lo, K.-Y. 1983, ApJ, 265, 711
Spekkens, K., Urbancic, N., Mason, B., Willman, B. & Aguirre, J. E. 2014, ApJ, 795, L5
Tollerud, E. J., Geha, M. C., Grcevich, J., Putman, M. E. & Stern, D. 2015, ApJ, 798, L21 (TOL15)
Tollerud, E. J., Geha, M. C., Grcevich, J., Putman, M. E., Weisz, D. & Dolphin, A. 2016 , submitted to ApJ
Westmeier, T. et al. 2015, MNRAS, 453, 338
Wong, O.I. et al. 2006, MNRAS, 371, 1855